

## Multiple Ion Cores in Anthracene Anion Clusters\*\*

Jae Kyu Song, Nam Ki Lee, and Seong Keun Kim\*

Small aromatic hydrocarbons do not generally accommodate an excess electron to form a stable anion, and only transient anions of very short lifetime have been observed with shape resonance.<sup>[1]</sup> However, the decreasing value of the negative electron affinity with increasing ring size indicates that charge delocalization renders electron attachment to these molecules less prohibitive. For example, electron affinity changes from  $-1.12$  eV for benzene to  $-0.19$  eV for naphthalene.<sup>[1]</sup> Thus the large molecular framework of anthracene leads to sufficient delocalization of the excess electronic charge to give the molecule a *positive* electron affinity of  $0.53$  eV,<sup>[2]</sup> which makes it the smallest unsubstituted aromatic hydrocarbon with a stable valence anion state.

Anthracene has been studied as a prototypical model for a localized charge carrier system in organic molecular crystals over the last several decades.<sup>[3]</sup> A charge is known to be localized in these systems through a polarization-type interaction between the charge carrier and the local lattice environment. Since anthracene cluster anions can serve as a model for a microscopic charge-injected system, study of such anions will lead to a better understanding of the mechanism of electron localization as well as electron transfer in molecular crystals.

Another goal of this study concerns the elucidation of the ion core structure of aromatic anion clusters, of which little is known so far, in contrast to the case of aromatic cation clusters.<sup>[4–8]</sup> The cation dimer of benzene was found to form a unique ion core stabilized by what is known as charge resonance.<sup>[4–6]</sup> A similar case was also found for naphthalene and anthracene dimer cations.<sup>[4,7,8]</sup> The only sign of charge resonance observed for aromatic anions, however, was in the case of anthracene in bulk glassy solution,<sup>[9]</sup> where its anion was believed to exist as a dimeric unit.<sup>[9,10]</sup> Only very recently was the ion core of naphthalene anion clusters directly examined and found to have a monomeric charge core.<sup>[11]</sup>

In this study, we examined the ion core structure of small anthracene anion clusters,  $(\text{An})_n^-$  ( $n=1-6$ ), in the gas phase and found that  $(\text{An})_n^-$  can have monomeric, dimeric, and trimeric ion cores and thus undergoes multiple core switching as the cluster increases in size.

Two typical mass distributions of  $(\text{An})_n^-$  clusters obtained under different conditions are shown in Figure 1. Although the overall shapes of the distributions are different, both show a mild intensity anomaly at  $n=5$ , which may indicate structural stability resulting from shell closing, as in the case of benzene cluster cations, which have a magic number of  $n=14$ .<sup>[12]</sup> In order to investigate this possibility in more detail, photoelectron spectroscopy and theoretical calculations were carried out for  $(\text{An})_n^-$  clusters.

The photoelectron spectra of  $(\text{An})_1^-$  obtained at four different photon energies are presented in Figure 2. The photoelectron spectrum obtained at  $1064$  nm displays a well-resolved structure, with a separation of  $0.05$  eV (about  $400\text{ cm}^{-1}$ ), which most likely reflects the totally symmetric  $\nu_{12}$  vibrational mode ( $390\text{ cm}^{-1}$ ).<sup>[2,13]</sup> The fourth peak, at  $0.715$  eV, seems to belong to a different vibrational progression because its intensity is higher than the third peak and its spacing is incommensurate with the other peaks. The energy gap between the fourth peak and the origin is  $0.175$  eV ( $1410\text{ cm}^{-1}$ ), which probably represents another totally symmetric mode,  $\nu_6 = 1408\text{ cm}^{-1}$ .<sup>[13]</sup> The electron affinity of An was determined from the position of the origin band to be  $0.54$  eV, which agrees with the literature value of  $0.53$  eV.<sup>[2]</sup>

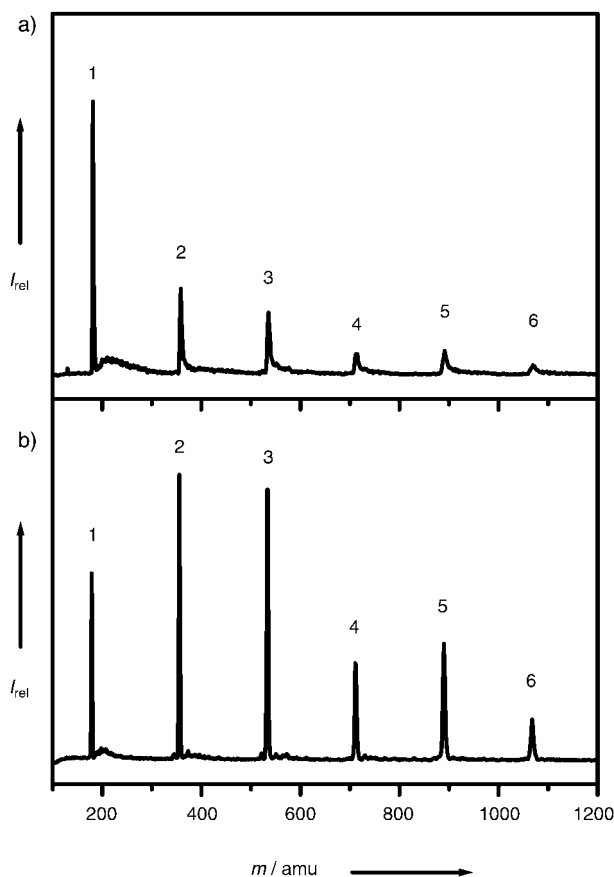


**Figure 1.** Mass distributions of the anthracene anion clusters,  $(\text{An})_n^-$ . The spectra were obtained under different conditions chosen to enhance (a) the smaller clusters and (b) the larger ones. Both show the magic number,  $n=5$ .

[\*] Prof. Dr. S. K. Kim, J. K. Song, N. K. Lee  
School of Chemistry  
Seoul National University  
Seoul 151-747 (Korea)  
Fax: (+82) 2-889-5719  
E-mail: seongkim@plaza.snu.ac.kr

[\*\*] This work was supported by the National Creative Research Initiatives Program (99-C-CT-01-C-50) of the Ministry of Science and Technology of Korea.

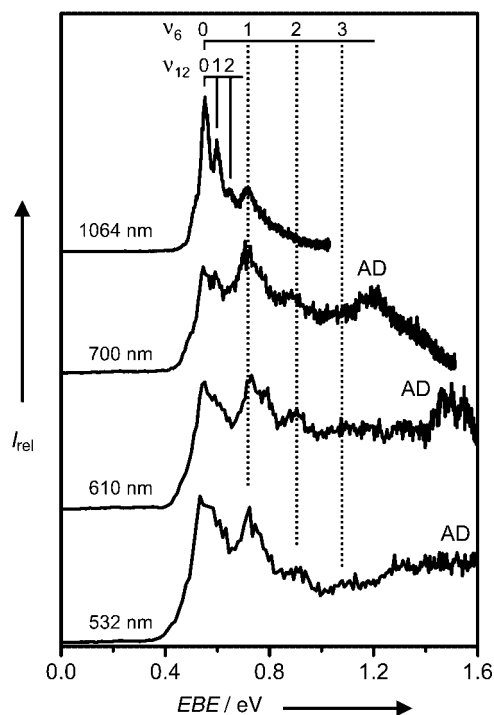


**Figure 2.** Photoelectron spectra of the anthracene monomer anion,  $(\text{An})_1^-$ , measured by photodetachment at 1064, 700, 610, and 532 nm. The slow rise beginning near 1.0 eV of the electron binding energy (EBE) in the bottom three spectra is tentatively ascribed to autodetachment from a short-lived excited state of the anthracene anion.

The hump at the rising part of the origin band may be ascribed to a hot band transition.

The photoelectron spectra obtained at other wavelengths display totally different peak shapes. The  $\nu_{12}$  mode is hardly discernable due to the limited resolution of our photoelectron spectrometer at these electron kinetic energies. Here, the only clearly identifiable vibrational progression is that observed for the  $\nu_6$  mode. The slow rise in electron binding energy beginning at 1.0 eV may be the result of autodetachment from a short-lived excited state of the An anion accessible at a photon energy above that at a wavelength of 700 nm.<sup>[1,9]</sup>

The photoelectron spectra of the entire series of  $(\text{An})_n^-$  ( $n=1-6$ ) clusters studied are presented in the left-hand column of Figure 3. It is evident that there is an irregular change of spectral profile at  $n=4$ . In order to better resolve the spectra, we deconvoluted them with a set of Gaussian peaks with an energy spacing equal to that of the  $\nu_6$  mode. The results are shown in the right-hand column of Figure 3 and yield a remarkably good fit over the entire series of  $(\text{An})_n^-$  clusters.

At first glance, the seemingly gradual shift of peaks from  $n=1$  to  $n=3$  appears to indicate a typical solvation effect, whereby each additional solvent molecule around a common central ion stabilizes the ion in a steady, stepwise manner. But, the very anomalous shape of the spectrum at  $n=4$  casts strong doubt upon this interpretation. The prospect of the failure of a simple solvation model involving a single common ion core prompted us to carry out theoretical calculations to address the character of the ions that give rise to the spectra in

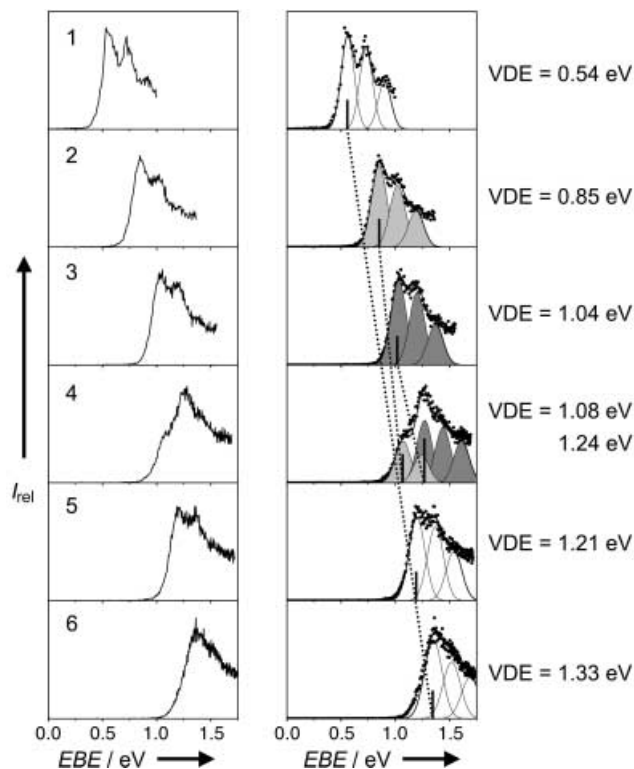


**Figure 3.** Left: photoelectron spectra of anthracene cluster anions,  $(\text{An})_n^-$  ( $n=1-6$ ), measured by photodetachment at 532 nm. Right: deconvolution of the spectra with a set of Gaussian functions with a fixed spacing equal to that of the  $\nu_6$  mode. The broad band produced by autodetachment was omitted for clarity. The solid bars denote the vertical detachment energies (VDEs) and the dotted lines connect the VDEs of anions with a common ion core (discussed in the text). The monomeric ion core at  $n=1$  is represented by unshaded curves, the dimeric core at  $n=2$  by light gray shading, and the trimeric core at  $n=3$  by dark gray shading. The spectra are plotted against electron binding energy.

Figure 3. We employed density functional theory (DFT) at the B3LYP/6-31G\* level by using the Gaussian 98 program suite.<sup>[14]</sup> Stable geometries were calculated by using analytical gradients with full geometry optimization. The frequencies of optimized geometries were obtained to make sure that these structures represent stable points on the potential energy surface.

The most stable geometry of the  $(\text{An})_2^-$  species was found to be a symmetric parallel-displaced (PD) structure, shown in Figure 4a. According to the charge population analysis, the excess electron is delocalized over the two moieties equally, which means that  $(\text{An})_2^-$  is a dimeric ion rather than an ion-solvent complex. It is also worth noting that the difference in VDE values between consecutive spectra in Figure 3 is by far the largest between  $n=1$  and  $n=2$ , and this difference is comparable to the energy gain expected for charge resonance.<sup>[14]</sup>

The structure of the  $(\text{An})_3^-$  cluster was also optimized by a DFT calculation at B3LYP/6-31G\*, which yielded the double parallel-displaced (DPD) geometry shown in Figure 4b as its most stable structure. In this geometry, the excess electron is quite evenly delocalized over the three molecules, with a little

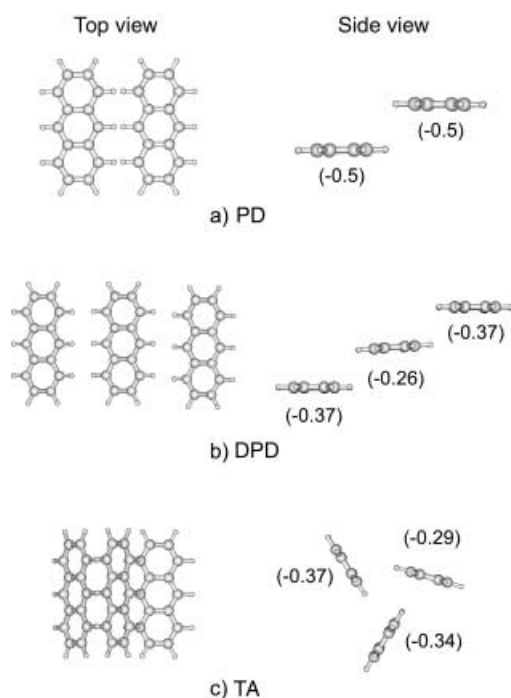


**Figure 4.** a) The most stable geometry of  $(\text{An})_2^-$ . b) The most stable geometry of  $(\text{An})_3^-$ . c) Another low-energy structure for  $(\text{An})_3^-$ . The numbers in parentheses represent the charge populations on each constituent molecule obtained by Mulliken population analysis.

more charge on the two end moieties than on the middle one. A careful inspection of the geometry also shows that the three molecules are not perfectly parallel; the middle molecule is slightly tilted to face the two end moieties. Another stable geometry for the  $(\text{An})_3^-$  species is the triangular (TA) geometry shown in Figure 4c, which is similar to the known stable geometry of aromatic neutral trimers.<sup>[15,16]</sup> This structure is somewhat asymmetric, unlike neutral trimers, which have a perfect symmetry. The TA geometry is 0.05 eV higher in energy than the DPD structure. The excess electron in the TA geometry is also quite evenly delocalized over the three moieties. In either case, we conclude that  $(\text{An})_3^-$  forms a trimeric ion core rather than an ion–solvent complex with a monomeric or dimeric ion core.

The monomeric, dimeric, or trimeric nature of the ion core is indicated by shading in the right-hand column of Figure 3. The seemingly composite nature of the band profile for the  $(\text{An})_4^-$  species and the anomalous origin band suggest coexistence of different ion cores, each with their own VDE value. The deconvolution of the photoelectron spectrum with dimeric and trimeric band components gave a surprisingly good fit, which suggests that  $(\text{An})_4^-$  exists in two forms:  $(\text{An})_2^--(\text{An})_2$  and  $(\text{An})_3^--(\text{An})_1$ , with a dimeric and a trimeric ion core, respectively. Recently it was reported that two stable geometries of the neutral  $(\text{An})_4$  species can also coexist with similar stability.<sup>[16]</sup> One of these geometries is built on a dimeric unit and the other on a trimeric unit.

In Figure 3, three dotted lines are drawn between anions with a common ion core in an attempt to connect the VDEs on the basis of a solvation model involving multiple ion cores.

The VDE of the dimeric  $(\text{An})_4^-$  ion is connected to that of  $(\text{An})_2^-$  by a line, while the VDE of the trimeric  $(\text{An})_4^-$  is connected to that of  $(\text{An})_3^-$ . The line connecting the VDEs of  $(\text{An})_5^-$  and  $(\text{An})_6^-$  leads directly to the VDE of  $(\text{An})_1^-$ , which may imply that these two anions have a monomeric ion core. This result, in addition to the observed magic number of  $n=5$ , may indicate a shell closure around a monomeric anion core by four solvent molecules, which suggests another core switching from  $n=4$  to  $n=5$ .

In summary, we found monomeric, dimeric, and trimeric anion core structures for the  $(\text{An})_n^-$  ( $n=1-6$ ) clusters. Different ion cores have their own characteristic VDE values, which are different from the values anticipated from a simple stepwise solvation model involving a single common ion core. Coexistence of a dimeric and a trimeric anion core was found in  $(\text{An})_4^-$ . A monomeric ion core structure is restored in  $(\text{An})_5^-$ , probably because of the enhanced stability that is associated with the completion of a solvation shell with four solvent molecules around the monomeric anion.

## Experimental Section

The details of our experimental apparatus have been reported elsewhere.<sup>[17,18]</sup> The molecular beam was generated by supersonic expansion of An vapor at 170°C seeded in Ar carrier gas. The anion clusters were first mass selected and then subjected to photoelectron spectroscopy with unfocused laser light at a fluence of 2 mJ pulse<sup>-1</sup> cm<sup>-2</sup> to achieve photodetachment but avoid multiphoton effects.<sup>[17,19]</sup>

Received: June 24, 2002 [Z19597]

- [1] P. D. Burrow, J. A. Michejda, K. D. Jordan, *J. Chem. Phys.* **1987**, *86*, 9.
- [2] J. Schiedt, R. Weinkauff, *Chem. Phys. Lett.* **1997**, *266*, 201.
- [3] E. A. Silinsh, V. Čápek, *Organic Molecular Crystals*, AIP, New York, **1994**.
- [4] M. Meot-Ner, *J. Phys. Chem.* **1980**, *84*, 2724.
- [5] H. J. Neusser, H. Krause, *Chem. Rev.* **1994**, *94*, 1829.
- [6] K. Ohashi, N. Nishi, *J. Chem. Phys.* **1998**, *109*, 3971.
- [7] H. Saigusa, E. C. Lim, *J. Phys. Chem.* **1994**, *98*, 13470.
- [8] Y. Inokuchi, K. Ohashi, M. Matsumoto, N. Nishi, *J. Phys. Chem.* **1995**, *99*, 3416.
- [9] T. Shida, S. Iwata, *J. Chem. Phys.* **1972**, *56*, 2858.
- [10] J. McHale, J. Simons, *J. Chem. Phys.* **1980**, *72*, 425.
- [11] J. K. Song, S. Y. Han, I. Chu, J. H. Kim, S. K. Kim, S. A. Lyapustina, S. Xu, J. M. Nilles, K. H. Bowen, *J. Chem. Phys.* **2002**, *116*, 4477.
- [12] B. Ernstberger, H. Krause, H. J. Neusser, *Ber. Bunsen-Ges.* **1993**, *97*, 884.
- [13] W. R. Lambert, P. M. Felker, J. A. Syage, A. H. Zewail, *J. Chem. Phys.* **1984**, *81*, 2195.
- [14] Gaussian 98 (Revision A.7), M. J. Frisch, G. W. Trucks, H. B. Schlegel, G. E. Scuseria, M. A. Robb, J. R. Cheeseman, V. G. Zakrzewski, J. A. Montgomery, R. E. Stratmann, J. C. Burant, S. Dapprich, J. M. Millam, A. D. Daniels, K. N. Kudin, M. C. Strain, O. Farkas, J. Tomasi, V. Barone, M. Cossi, R. Cammi, B. Mennucci, C. Pomelli, C. Adamo, S. Clifford, J. Ochterski, G. A. Petersson, P. Y. Ayala, Q. Cui, K. Morokuma, D. K. Malick, A. D. Rabuck, K. Raghavachari, J. B. Foresman, J. Cioslowski, J. V. Ortiz, A. G. Baboul, B. B. Stefanov, G. Liu, A. Liashenko, P. Piskorz, I. Komaromi, R. Gomperts, R. L. Martin, D. J. Fox, T. Keith, M. A. Al-Laham, C. Y. Peng, A. Nanayakkara, C.

- Gonzalez, M. Challacombe, P. M. W. Gill, B. G. Johnson, W. Chen, M. W. Wong, J. L. Andres, M. Head-Gordon, E. S. Replogle, J. A. Pople, Gaussian, Inc., Pittsburgh, PA, 1998.
- [15] C. Gonzalez, T. C. Allison, E. C. Lim, *J. Phys. Chem. A* **2001**, *105*, 10583; C. Gonzalez, E. C. Lim, *J. Phys. Chem. A* **1999**, *103*, 1437; C. Gonzalez, E. C. Lim, *Chem. Phys. Lett.* **2002**, *357*, 161.
- [16] F. Piuze, I. Dimicoli, M. Mons, P. Millié, V. Brenner, Q. Zhao, B. Soep, A. Tramer, *Chem. Phys.* **2002**, *275*, 123.
- [17] S. Y. Han, J. K. Song, J. H. Kim, H. B. Oh, S. K. Kim, *J. Chem. Phys.* **1999**, *111*, 4041.
- [18] J. K. Song, N. K. Lee, S. K. Kim, *J. Chem. Phys.* **2002**, *117*, 1589.
- [19] J. Schiedt, R. Weinkauf, D. M. Neumark, E. W. Schlag, *Chem. Phys.* **1998**, *239*, 511.

## Migration/Redistribution

# Polyhydrido(silylene)osmium and Silyl(dinitrogen)ruthenium Products Through Redistribution of Phenylsilane with Osmium and Ruthenium Pincer Complexes\*\*

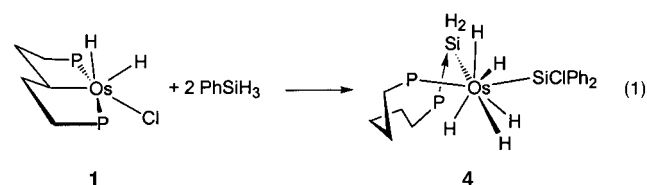
Dmitry G. Gusev,\* Frédéric-Georges Fontaine,  
Alan J. Lough, and Davit Zargarian\*

Transition-metal silylene complexes, silicon analogues of metal carbenes, are reactive species believed to be important intermediates in the industrial synthesis of chloromethylsilanes,<sup>[1]</sup> the catalytic oligomerization of hydrosilanes,<sup>[2]</sup> and the redistribution chemistry of organosilanes.<sup>[3]</sup> The high reactivity of metal silylenes is related to the electron deficiency of the silicon center, which is presumably due to the very weak  $\pi$  bonding between the silicon atom and the transition metal.<sup>[4]</sup> Consistent with this notion, in most of the

complexes reported to date<sup>[5]</sup> the silylene moiety requires stabilization from coordinating Lewis bases and/or heteroatom-based substituents (e.g., OR, SR, NR<sub>2</sub>),<sup>[6]</sup> whereas nonstabilized silylene complexes are difficult to isolate.<sup>[7]</sup>

The tendency of Os and Ru pincer complexes to give coordinatively unsaturated alkylidene and vinylidene products in reactions with alkynes<sup>[8a]</sup> prompted us to investigate their reactivity towards hydrosilanes with the expectation that addition or 1,2 migration of the Si–H bonds might afford silylene products. Here we describe silylene and silyl complexes obtained from the reaction of PhSiH<sub>3</sub> with [OsH<sub>2</sub>Cl{CH(C<sub>2</sub>H<sub>4</sub>PrBu<sub>2</sub>)<sub>2</sub>}] (**1**),<sup>[8b]</sup> [OsH<sub>2</sub>Cl{2,6-(CH<sub>2</sub>PrBu<sub>2</sub>)<sub>2</sub>C<sub>6</sub>H<sub>3</sub>}] (**2**),<sup>[8c]</sup> and [RuHCl{1,3-(CH<sub>2</sub>PrBu<sub>2</sub>)<sub>2</sub>-C<sub>6</sub>H<sub>4</sub>}] (**3**).<sup>[8d]</sup>

Addition of 2 equiv of PhSiH<sub>3</sub> to **1** in toluene afforded the pentahydrido complex **4** in 83 % yield [Eq. (1), P = PrBu<sub>2</sub>]. A



single-crystal X-ray analysis of **4** showed that the Os center adopts an 8-coordinate, dodecahedral geometry consisting of two orthogonal, trapezoidal planes defined by the atoms Si1, H1<sub>Os</sub>, H5<sub>Os</sub>, P2 and Si2, H3<sub>Os</sub>, H4<sub>Os</sub>, H2<sub>Os</sub> (Figure 1, left). The Os–Si distances for the silyl (2.374 Å) and the base-stabilized silylene (2.386 Å) ligand are in the normal range for Os–Si single bonds in hydrido(silyl)osmium complexes (3.34 to 2.49 Å).<sup>[9]</sup> The anticipated uncertainty associated with locating the hydride ligands in the solid-state structure of **4** prompted a study of its structure using ONIOM (DFT/HF) geometry optimization (Figure 1, right);<sup>[10]</sup> the closeness of the computational and experimental data indicates that the structure of this complex has been established reliably. Solution NMR data are also consistent with the proposed structure for **4** and show that the hydride ligands are highly fluxional. For example, the averaged OsH<sub>5</sub> resonance did not decoalesce down to –100 °C (<sup>1</sup>H NMR, [D<sub>8</sub>]toluene) and its

